KnE Engineering

ICEUBI2019
International Congress on Engineering — Engineering for Evolution
Volume 2020

Knowledge E
enriching | engaging | empowering

Conference Paper

Prediction of Pollutants Emissions in a CFM56-3 Combustor, Using Large Eddy Simulation

Inês Isabel Ascensão Costa Morão[1] and Francisco Miguel Ribeiro Proença Brojo[2]

[1]Universidade da Beira Interior
[2]C-MAST

Abstract

In the present work a CFD simulation was performed using a CFM56-3 combustor. It was intended to simulate the combustion and emission of pollutants (CO2, CO, UHC and NOx) from the different jet fuels (Jet A, Jet B and TS-1), when burning these through ICAO's LTO cycle. Being this a continuity study, the CAD model of CFM56-3 made by Oliveira [5] was used. The mesh was constructed with HELYX-OS software and the numerical study was made using the commercial software ANSYS Fluent 16.2. It can be concluded, amongst all the fuels simulated that increasing the power produces higher NOx. There was also an erratic behaviour in the emissions of UHC and CO results, because an empiric model was used and not a detailed chemical model.

Keywords: Jet Fuels, ANSYS Fluent, Pollutants emissions, ICAO's LTO cycle, CFM56-3

Corresponding Author:
Inês Isabel Ascensão Costa Morão
ines.morao.96@gmail.com

Received: 26 November 2019
Accepted: 13 May 2020
Published: 2 June 2020

Publishing services provided by Knowledge E

Selection and Peer-review under the responsibility of the ICEUBI2019 Conference Committee.

OPEN ACCESS

1. Introduction

During the past decade, the consumption of fuel by civil aviation has increased to the extent that air transport is now perceived as one of the world's fastest growing energy-use sectors [1]. Worldwide demand of jet fuel has been steadily increasing since 1980 [2]. Consumption more than tripled in 30 years from 1,837,000 barrels/day in 1980, to 5,220,000 in 2010.

Emissions resulting from the combustion of fossil fuels are usually considered as the main responsible for Greenhouse Gas (GHG) emissions, which are appointed as the primary factor that leads to global warming [3]. There are two main sources of aircraft emissions, the jet engines and the auxiliary power unit (APU). Most jet fuel is burned in flight so most of the emissions occur at altitude, not at ground level. Therefore, it has a significant impact both on local air quality and global atmospheric changes, which leads to the introduction of more drastic regulations of pollutant emissions [4].

There are technology and practical solutions to reduce the amount of heat-trapping emissions resulting from the continued increase in traffic in the aviation industry [5]. For example, changes in the structure of aircraft have been held to decrease fuel consumption thus reducing the emissions of GHG [5]. An example of this is the blended winglets, the new design feature in the wing tips. In the blended winglets the drag is reduced which consequently increases fuel efficiency [5].

The exhaust gases from an aircraft gas turbine are composed of carbon monoxide (CO), carbon dioxide (CO_2), water vapor (H_2O), unburned hydrocarbons (UHC), particulate matter (mainly carbon), NO_x, and excess atmospheric oxygen and nitrogen [1]. Carbon dioxide and water have not always been regarded as pollutants because they are the natural consequence of complete combustion of a hydrocarbon fuel [1]. However, they both contribute to global warming and can only be reduced by burning less fuel [1].

Aircraft engines have two quite different requirements [6]. The first is for very high combustion efficiency at low power, because of the large amounts of fuel burned during taxiing and ground manoeuvring. The primary problem here is the reduction of UHC [6]. At take-off power, climb and cruise the main concern is NO_x [6]. The International Civil Aviation Organization (ICAO) sets standards on a worldwide basis, for both the take-off and landing cycles and also for cruise at high altitude; the first is concerned with air quality in the vicinity of airports and the second with ozone depletion in the upper atmosphere [6].

Within the context mentioned previously, the work presented in this paper has as main objective to simulate the combustion and emission of pollutants from the major civil jet fuels grades (Jet A, Jet B and TS-1) in a CFM56-3 combustor, while burning them through ICAO's LTO (landing and take-off) cycle.

To achieve the objective described previously was necessary to:

1. Understand the process of combustion and formation of pollutants in annular chambers;

2. Select usual fuels and engine operating points (take-off, cruise, approach and idle);

3. Simulate the combustion of the various fuels at the operating points considered;

4. Perform a comparative study of the various fuels results;

5. Analyze the flow and estimate reasons for possible malfunctions.

2. Bibliographic Review

2.1. Combustor

The goal of the combustor is to convert the chemical energy bound in the fuel into thermal energy, that will be used by the turbine to produce the power required to operate the various stages of compressors and/or fans. It is important to understand the difference between the Combustor Chamber (CC) and the combustor. The combustor is composed by the diffuser, the combustion chamber, the inner and outer casing, the spark plugs and the fuel injectors. The Combustor chamber refers to the exact place in which combustion takes place [5].

The combustor is a critical component in the GTE (gas turbine engine), because it must operate reliably at extreme temperature and it must produce a minimum amount of pollutants over a long operating life [5]. Figure 1 shows the CFM56-3 combustor during the digitalization process to obtain the geometry.

Figure 1: CFM56-3 combustor photograph. (Source: [5]).

There are three types of combustor chambers: tubular (also known as “can”), annular and the “tuboannular” (also known as “can-annular”).The choice of a particular type and layout of combustion chamber is determined largely by engine specifications, but it is also strongly influenced by the desirability of using the available space as effectively as possible [1].

Tubular combustors have the simplest form for the combustor and were used in early jet engines. Most of the early jet engines features tubular chambers, usually in numbers varying from eight to sixteen per engine, and even today a single of low power output. However, for the big majority of aircraft applications, the tubular system is too long and heavy and results in an engine of large frontal area and high drag [7].

The tubo-annular chamber comprises a group of cylindrical flame tubes arranged inside a single annular casing. It represents an attempt to combine the compactness of the annular chamber with the best features of the tubular system. Compared with the annular design the tubo- annular chamber has an important advantage in that much useful chamber development can be carried out with very modest air supplies, using just a small segment of the total chamber containing one or more flame – tubes [7].

The annular configuration is used by most modern jet engines because of its lighter design. The CFM56-3 combustor has an annular configuration. In this type an annular flame-tube is mounted concentrically inside an annular casing. The annular combustor arrangement is illustrated in Figure 2. It is an ideal form of chamber since its ”clean” aerodynamic layout result in a compact unit of lower pressure loss than other camber design. Unfortunately, one undesirable outcome of the annular system’s excellent aerodynamic characteristics is that a slight variation in the velocity profile of the inlet air can produce a significant change in the temperature distribution of the outlet gases [7].

Another problem with large annular chambers stems from the heavy buckling load on the outer flame-tube. Distortion of the flame-tube disrupt the flow of cooling air and also changes the outlet temperature distribution. Test-bed development of annular chambers presents serious difficulties because there are very few facilities anywhere in the world that can supply air at the levels of pressure and temperature and in the amounts required to test large annular combustion chambers at take-off conditions. Here is a new field for research. In the past considerable time and ingenuity was spent in devising methods of simulation low combustion pressure in order to reproduce combustion conditions corresponding to high altitudes. Today, with the trend towards more widespread use of annular designs, the urgent need is for methods of simulating high combustion pressures in chambers that are actually operating at lower and more convenient level of pressure [7].

2.2. Jet Fuel

At the current time, almost all aviation fuel (jet fuel) is extracted from the middle distillates of crude oil (kerosene fraction), which distils between the gasoline and the diesel

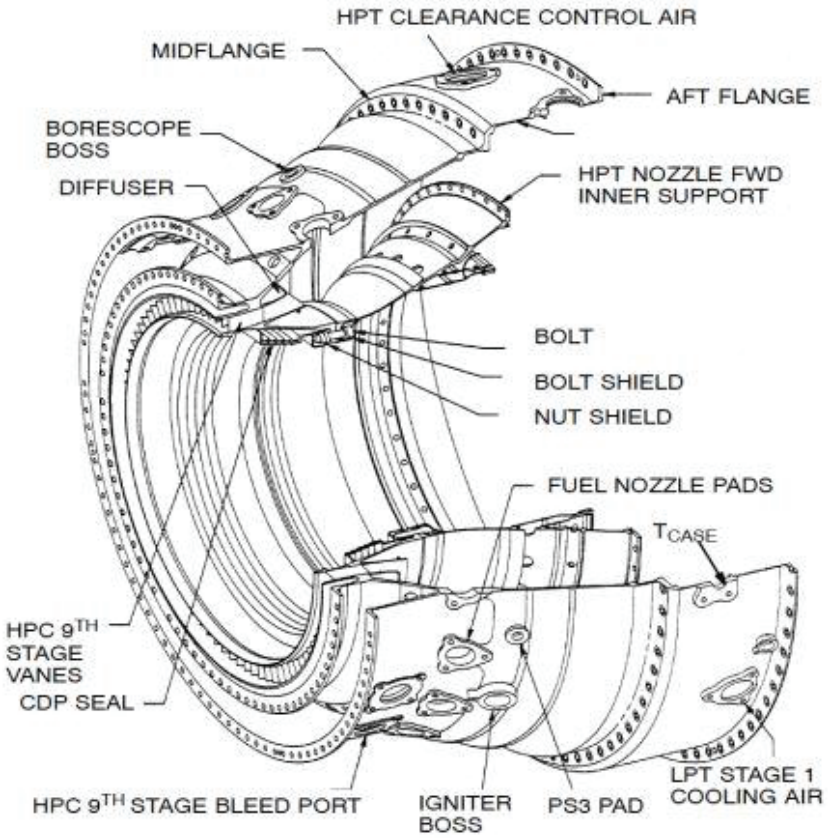

Figure 2: Annular combustor arrangement. (Source: [8]).

fractions [9]. The kerosene-type fuels most used worldwide in civil aviation are of Jet A and Jet A-1 grades: Jet A is used in most of the world, except North America where Jet A-1 is used [9]. Jet A-1 has same flash point as Jet A but a lower freeze point.

Other fuels can be used as an alternative to Jet A-1. Jet B is a wide-cut type fuel covering both the naphtha and kerosene fractions of crude oil and is used in very cold climates, e.g. in northern Canada where its thermodynamic characteristics (mainly lower freeze point and higher volatility) are suitable for handling and cold starting [9].

TS-1 is the main jet fuel grade available in Russian and CIS states; it is a kerosene-type fuel with slightly higher volatility and lower freeze point compared to Jet A and A-1 fuels [9].

The main fuel used in China is RP-3 (renamed No 3 Jet Fuel) and is basically as Western Jet A- 1, produced as an export grade [10].

2.3. Combustion Stoichiometry

Two components, the fuel and the oxidant, are required for combustion. In case of combustion of a hydrocarbon (C_xH_y) there is always formation of CO_2 and H_2O, and the stoichiometric reaction is defined by the Eq (1):

$$C_xH_y + \left(x + \frac{y}{4}\right) O_2 \rightarrow xCO_2 + \frac{y}{2}H_2O \quad (1)$$

There are two types of combustion, complete and incomplete. The difference between these two types of combustion lies in the products of the reaction. In the complete combustion is only released CO_2, H_2O and energy and in the incomplete reaction is released CO_2, H_2O, intermediary products (CO, etc.) and energy.

Air is composed in its majority by N_2 (76.8%), O_2 (23.2%), and small amounts of CO_2, argon and other traces of species. This means that for every mole of oxygen required for combustion, 3.76 mol of N_2 must be also introduced. N_2 does not alter significantly the O_2 balance, however it does have a major impact on the thermodynamics, chemical kinetics, and formation of pollutant in combustion systems [11]. This said, the complete stoichiometric relation for complete oxidation of a hydrocarbon fuel is represented in Eq (2):

$$C_xH_y + \left(x + \frac{y}{4}\right)(O_2 + 3.76N_2) \rightarrow xCO_2 + \frac{y}{2}H_2O + 3.76\left(x + \frac{y}{4}\right)N_2 \quad (2)$$

The emissions during standardised LTO cycles are then reported as emission index (EIs) expressed as mass of pollutant emitted per unit mass of fuel burned.

3. Flow Simulation

3.1. Geometry

All the details present in the combustor geometry are represented in Figure 3, including the combustor walls, dome, dilution holes, fuel injectors and primary/secondary swirlers. However, due to the existing symmetry, only a quarter section of this combustor was used for simulation purposes to decrease the simulation time. There is a fuel injector within the five fuel injectors, that supply a richer mixture to the combustor.

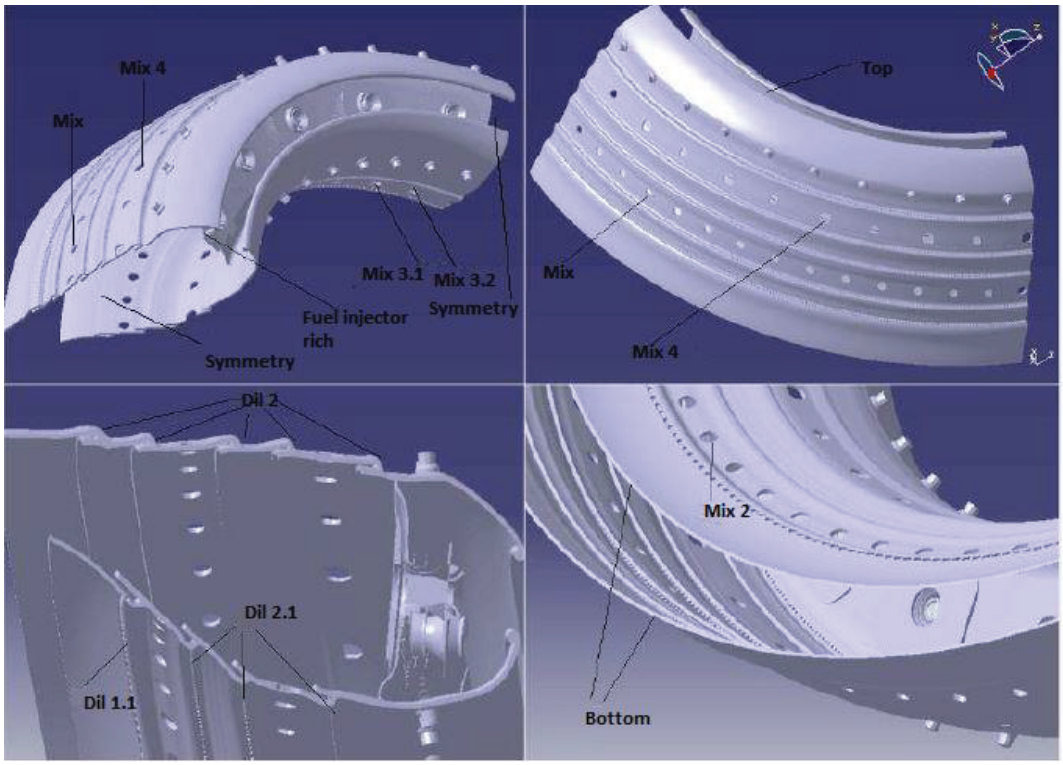

Figure 3: Views of the CAD combustor model section used in the simulations. (Source: [5]).

3.2. Mesh

The mesh generation was performed using HELYX-OS. This software has some advantages over other software's, as a quicker mesh generation time and a user-friendly software which enables the user to better refine any given part of the mesh. The obtained mesh has more than 4 million points and took about 8000 seconds to calculate. The mesh used has an aspect ratio of 1, which is the recommend in LES approach [12].

LES approach is very demanding in terms of computational power. Geometry used was very complex, creating many difficulties in the development of a more refined mesh. Figure 4 shows the final mesh used.

3.3. Numeric Simulation

The software used to perform this simulation was ANSYS Fluent 16.2. For the setup, the energy model was enabled. This model must be activated as this regards the energy related to the temperature change within the combustion process or heat transfer [5]**.** LES (large eddy simulation) was the chosen viscous model. Concerning heat transfer by radiation was chosen the Discrete Ordinates (DO) radiation model, because produces a more accurate solution than the P1 radiation model, but its drawback is a higher CPU

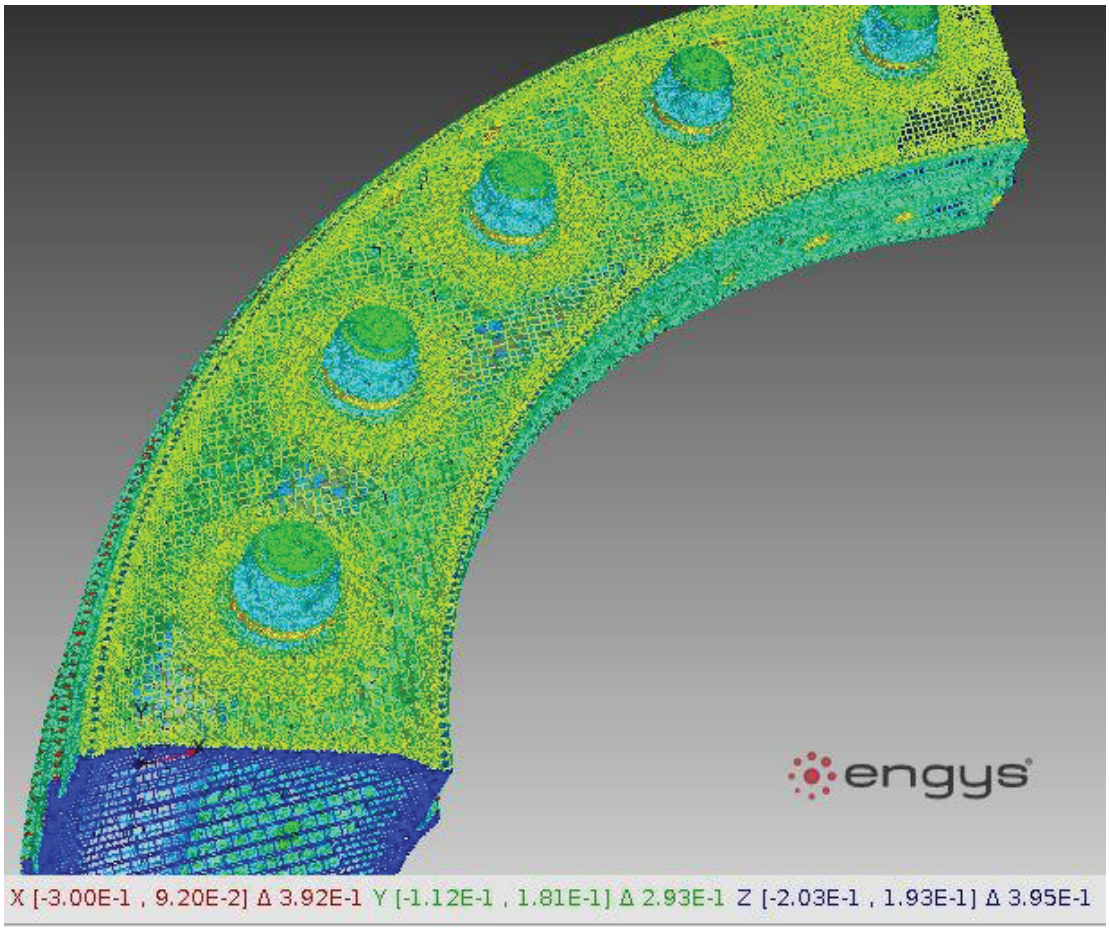

Figure 4: Final mesh, Software HELYX-OS.

cost [12]. The non-premixed combustion was used in the present simulation. The NO_x model was enabled to ANSYS Fluent display information regarding NO_x formation when the solution is calculated. The discrete phase model was also enabled. Concerning fuel injection, was considered the solid cone model.

It was obtained through the Ribeiro work [13] important aspects regarding each stage of the GTE, namely $\dot{m}_a$, temperature and pressure, at full power. Typical values for GTE's operating AFR are stated by Bryn Jones [14] and are between 33-40 at 100% power, and approximately 100 at 7% power.

The air that enters the PZ is done through the primary and secondary swirlers, and as so its mass flow rate can then be determined. Knowing the overall AFR and fuel flow, it is possible to determine the total $\dot{m}_a$ and then calculate the total cooling $\dot{m}_a$, by subtracting the PZ $\dot{m}_a$ from the total $\dot{m}_a$. The determination of which percentage of cooling air, to apply in each boundary was only possible through an extensive trial and error approach through the simulations, in which the aim was to achieve the exit temperature [5].

The recommended choice for the momentum equation is the Bounded Central Difference scheme, especially for complex geometries and flows [15]. Least Square Cell Based gradient method is essential in ANSYS Fluent [12], as it allows a better representation of the second derivative of the velocity field that is required for the model formulation (von Karman length scale) [15]. Solver selected was Coupled to the Pressure-Velocity Coupling. This solver is the recommended by ANSYS Fluent [12] when large time steps are used to solve the transient flow. The Bounded Second Order Implicit formulation was selected to temporal discretization. This solver provides better stability and improves accuracy [12].

4. Results

4.1. Oxides of nitrogen emissions

NO_x can be produced by two different mechanisms: thermal NO_x and prompt NO_x.

The thermal NO_x is the leading mechanism for NO_x formation at the high temperatures of the PZ, and prompt NO_x is only formed in fuel rich regions.

Oxides of nitrogen emissions are insignificant at low power settings and attain maximum values at the highest power condition.

As can be seen in Figure 5, NO_x emissions presented a little margin of error compared with the reference values presented by ICAO. However, in general, it was obtained good approaches to the reference values.

Still in Figure 5, it can be verified that Jet A presented the lowest value of EI NO_x) at cruise and TS-1 presented the highest value of EI (NO_x), at take-off.

Overall, it is possible to conclude that Jet B presented the lowest values of EI (NO_x) at take- off, approach and idle.

The results of EI (NO_x), present in Figure 6, consider the thermal NO_x and prompt NO_x that reached the combustor's exit.

The high peak temperatures are located within the PZ, but the oxidation occurs mainly in the post flame zone area, in which the concentration of the radicals O and OH are sufficient for the process to occur [16]. This statement is proved by analysing Figure 6; here the major concentrations of NO_x, are in the post-flame zone, and near the combustor's exit.

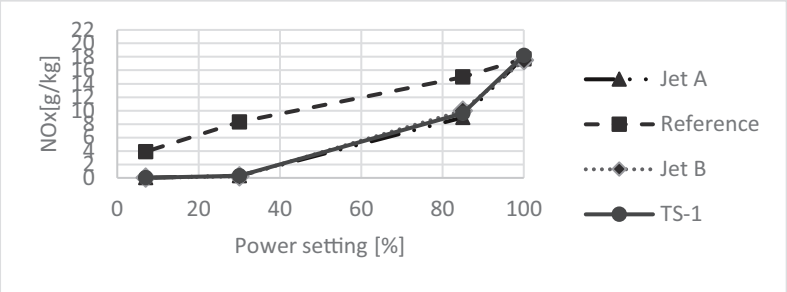

Figure 5: EI results of NOx, resultant from the combustion of Jet A, Jet B and TS-1, throughout ICAO's LTO cycle.

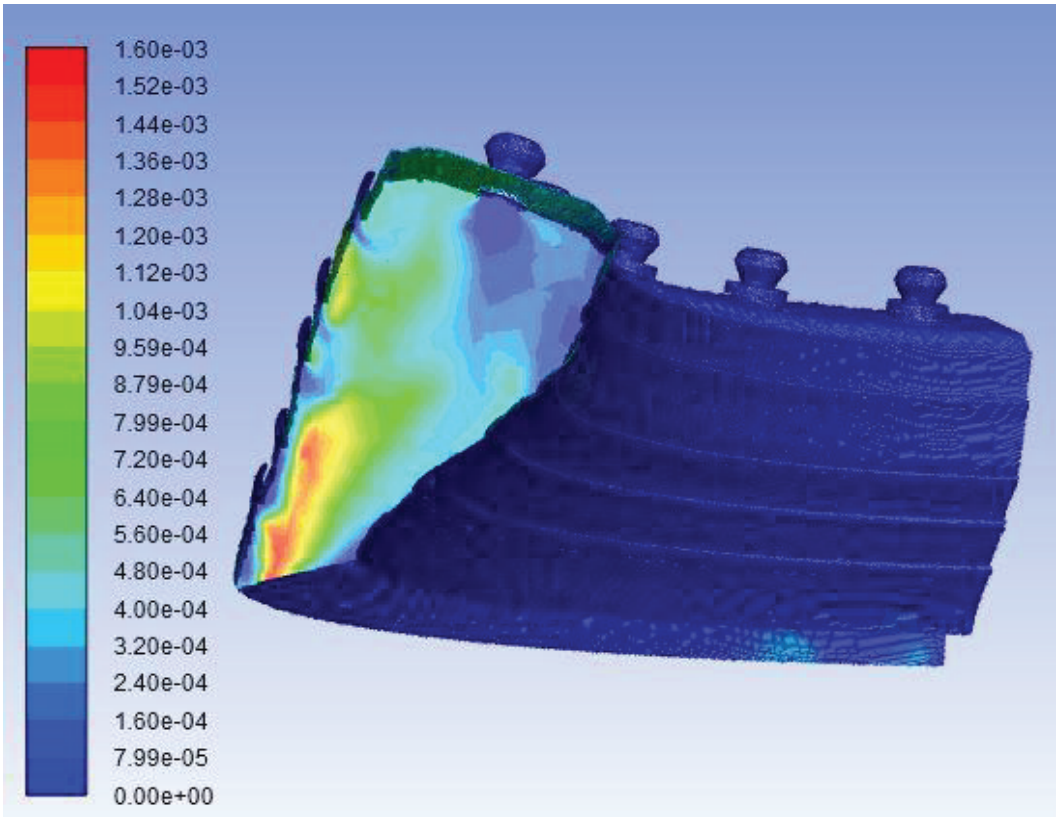

Figure 6: Contours of NOx concentration [kg/kg] at 85% power, while burning Jet A.

4.2. Carbon monoxide and Unburned hydrocarbons emissions

Carbon monoxide and unburned hydrocarbons emissions index are highest at low power settings where combustor temperatures and pressures are low, and combustion is less efficient [17].

As can be seen in the Figure 7 and 8, the results obtained present an irregular behaviour. The explanation for this behaviour was found in the EMICOPTER project [18]. The chemistry model used was an empiric model. The empirical models are used for correlating experimental data on pollutant emissions in terms of all the relevant parameters. These include combustor dimensions, design features, and operating conditions,

as well as fuel type and fuel spray characteristics. The empirical models predict NO_x emissions correctly, but in relation to CO and UHC emissions they do not have a good prediction, because the chemical reactions governing the formation of UHC and CO are highly complex.

A solution that was found and can be performed in future work is the use of a detailed chemistry model.

Analysing the figure 7, all the fuels maximum CO EI predicted throughout the cycle differ with the maximum reference values. Thus, all the fuels minimum CO EI predicted throughout the cycle differ with the minimum reference values. Still in Figure 7, it can be verified that Jet A presented the lowest value of EI(CO) at cruise, approach and idle.

Analysing Figure 8, it can be verified that Jet B presented the lowest EI (UHC) at full power and TS-1 presented the highest EI (UHC), at cruise. Still in Figure 8, it can be verified that all the fuels presented the same EI (UHC) values at approach and idle.

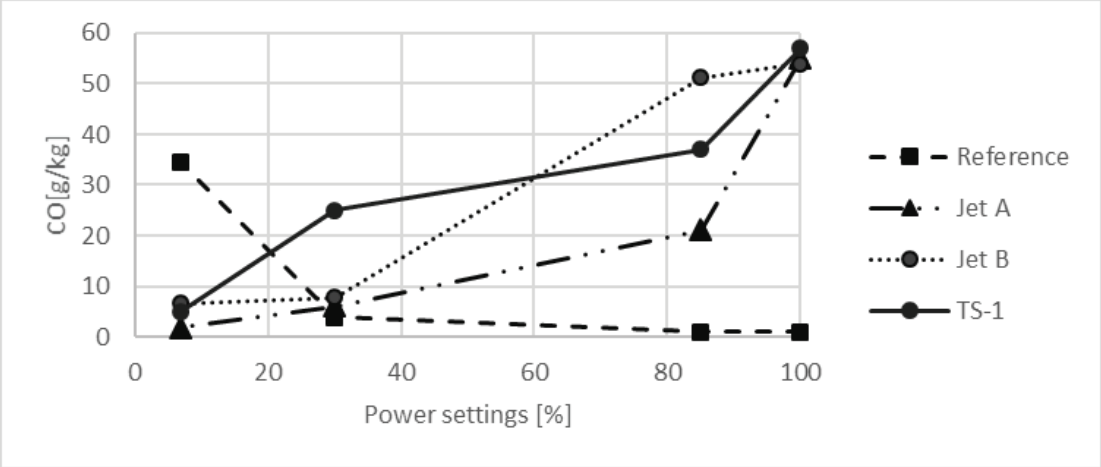

Figure 7: EI results of CO, resultant from the combustion of Jet A, Jet B and TS-1, throughout ICAO's LTO cycle.

Another weakness of the empirical model is that it cannot captur the quenching effect due to the cooling air near the walls on CO oxidation reactions, as can be seen in Figure 9. In fact, CO emissions are, at least partially, the effect of CO from the primary zone being entrained in the cool air along the liner where it fails to oxidize because of the low temperatures [18].

4.3. Carbon dioxide emissions

Carbon dioxide is recognised as the main greenhouse gas and has a primary role in the Earth's climate warming [9]. Typically, the EI (CO_2) from modern aircraft engines is 3160 $\pm$ 60 g/kg$_{fuel}$ for complete combustion [9]. However, some studies reported that

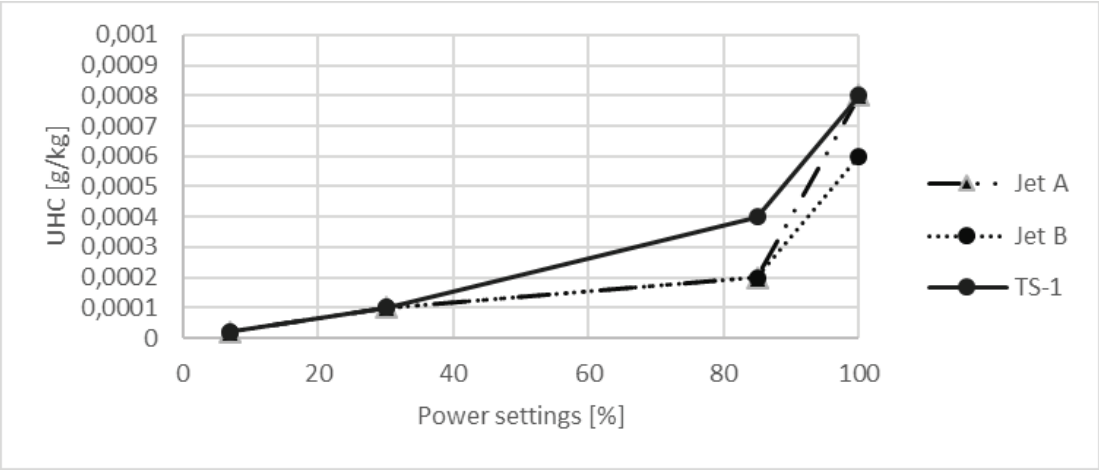

Figure 8: EI results of UHC, resultant from the combustion of Jet A, Jet B and TS-1, throughout ICAO's LTO cycle.

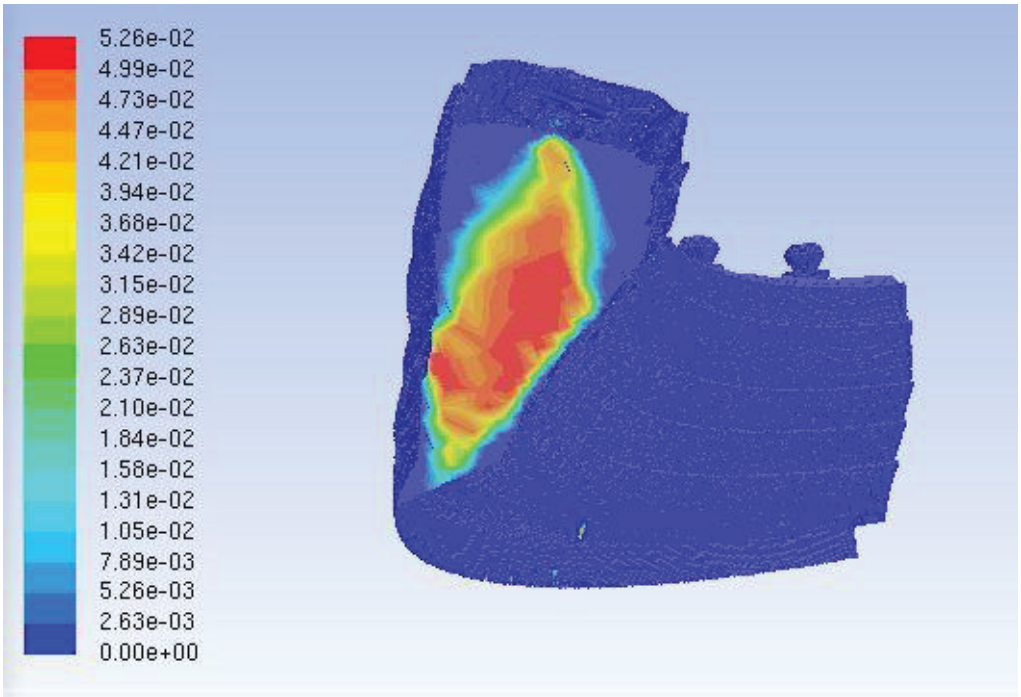

Figure 9: Contours of CO concentration [kg/kg] at full power, while burning Jet A.

EI (CO_2) decreases slightly at low thrust because incomplete combustion may result in a relative increase of CO and hydrocarbons in the exhaust [9].

Analysing the Figure 10, the results agree with what was said previous and the emission data indicate that the EI of CO_2 was the largest among the emissions considered; this behaviour is expected as CO_2 along with H_2O makes up great part of the exhaust gases. Still in Figure 10, Jet-A presented the highest value of EI (CO_2) and TS-1 presented the lowest value of EI (CO_2), at full power. TS-1 presented the lowest value of EI (CO_2), throughout ICAO's LTO cycle.

Overall, Jet-A presented the highest values of EI (CO_2), throughout ICAO's LTO cycle.

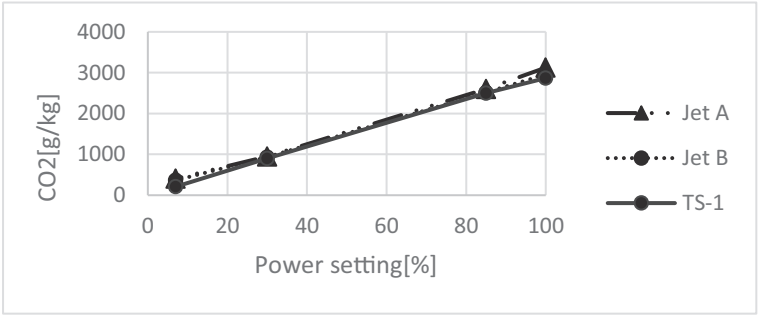

Figure 10: EI results of CO_2, resultant from the combustion of Jet A, Jet B and TS-1, throughout ICAO's LTO cycle.

In Figure 11, can be verified, that CO_2 is formed mostly in the flame zone and extends to the post-flame zone. This observation agrees with Lieuwen et al. [19].

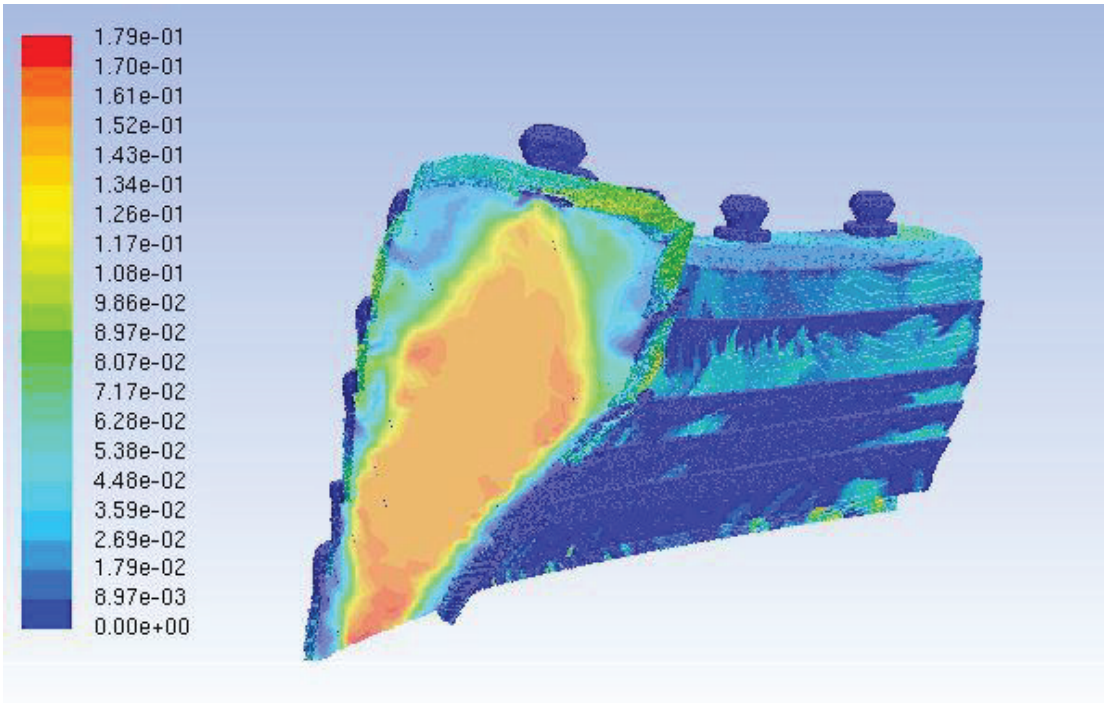

Figure 11: Contours of CO_2 concentration [kg/kg] at full power, while burning Jet A (a) and TS-1 (b).

5. Conclusions

Regarding the results, NO_x emissions presented a little margin of error compared with the reference values presented by ICAO. However, in general, it was obtained a good approach to the reference values. CO and UHC emissions exhibit erratic behaviour. After some research was found the reason; It was due to the chemical model used.

It was possible to conclude that Jet B presented the lowest values of EI (NO_x) at take-off, approach and idle. Jet A presented the highest values of EI (NO_x) at approach and idle.

Jet B presented the lowest values of EI (CO), at take-off and approach. Jet A presented the lowest values of EI (CO), at cruise and idle.

TS-1 presented the highest values of EI (UHC), at take-off and cruise. All fuels presented the same values of EI (UHC) at approach and idle.

TS-1 presented the lowest values of EI (CO_2) throughout the entire ICAO´s LTO cycle.

Acknowledgments

The current study was funded in part by Fundação para a Ciência e Tecnologia (FCT), under project UID/EMS/00151/2013 C-MAST, with reference POCI-01-0145-FEDER-007718.

References

[1] Lefebvre A.H.,and Ballal D. R., *Gas turbine combustion*, pp. 9, 359, 360, CRC Press, Boca Raton, United States Of America, 2010

[2] Muhammed, E. *Gas Turbine Fuels.* https://prezi.com/xstmwvtocpxn/gas-turbine-fuels/ (30 /7 /2019).

[3] The European Commission, “Climate change: commission proposes bringing air transport into EU emissions trading scheme.,” Brussels,Belgium, 2006.

[4] Jaravel, M. T., *Prediction of Pollutants in Gas Turbines using Large Eddy Simulation*, Ph.D. Dissertation, Polytechnique de Toulouse (INP Toulouse): Institut National Doctorat de l’université de Toulouse, Toulouse, France, 2016.

[5] Oliveira, J.,*CFD Analysis of the Combustion of Bio-Derived Fuels in the CFM56-3 Combustor,Master’s Thesis,* Universidade da Beira Interior, Covilhã,Portugal, 2016.

[6] Saravanamuttoo, H. I. H., Rogers, G. F. C., and Cohen, H. , *Gas turbine theory*,p. 292,Pearson Education, India, 2009.

[7] Smith, I. E., “Combustion in Advanced Gas Turbine Systems,” in *Proceedings of an International Propulsion Symposium Held at the College of Aeronautics*, Cranfield, England, UK, 1967.

[8] Aubuchon, D., Campbell, J., *CFM56-3 Turbofan Engine Description*, p. 19, Seneca College,India, 2006.

[9] Masiol, M. and Harrison, R. M,"Aircraft engine exhaust emissions and other airport-related contributions to ambient air pollution: A review," *Atmospheric Environment,* Vol. 95 (May 2014), pp. 409-455.

[10] Shell Global, *Civil Jet Fuel.* https://www.shell.com/business-customers/aviation/aviation-fuel/civil-jet-fuel-grades.html. (15 /7 /2019).

[11] Flagan,R.C. and Seinfeld,J.H., *Fundamentals of air pollution engineering*, pp. 42,45, Courier Corporation, Mineola, NY, USA, 2013.

[12] ANSYS, Inc, "ANSYS FLUENT 12.0/12.1 Documentation," 2009.

[13] Ribeiro P., *Análise de performance da Família de Motores de Avião CFM56*, pp. 65,66,73,102, Master's thesis, Instituto Superior de Engenharia de Lisboa,Lisboa, Portugal, 2012.

[14] Jones, B., *Gas Turbine Combustion*, pp. 28, 38, 41, 66, Cranfield University, Cambridge, England, UK, 2015.

[15] Menter, F.R., *ANSYS Germany GmbH, Best Practice: Scale-Resolving Simulations in ANSYS CFD Version 1.0*, Ansys inc, 2012.

[16] Zeldovich, Y. B., "The oxidation of nitrogen in combustion and explosions," *Acta Physicochim,URSS,* Vol. 21, n° 4 (1946), p. 577–628.

[17] Sutkus, D.J.Jr., Baughcum, S.L., DuBois, D.P., *Scheduled Civil Aircraft Emission Inventories for 1999: Database Dev. and Anal. NASA/CRm2001-211216*., 2001.

[18] The European Commission , Emicopter report summary. http://cordis.europa.eu/result/rcn/143538_en.html. (24 /7 /2019).

[19] Lieuwen, T.C. ,and Yang, V., Gas turbine emissions, , Cambridge University Press, Cambridge, Vol. 38 (2013) .